The effects of ultrasonic parameters on pressure fields in a membrane cleaning application

F. Reuter, R. Mettin, W. Lauterborn
Universität Göttingen, Drittes Physikalisches Institut, Germany, Email: f.reuter@physik3.gwdg.de

Introduction

Investigations of the cleaning of filtration membranes with ultrasound have been reported repeatedly [2, 3, 4, 5]. Nevertheless, only scattered details are known about the cleaning mechanisms, and theories that could help adapting ultrasonic and geometric parameters are missing. In this work, the cleaning of polymer flat sheet membranes that are built into a laboratory water filtration plant is investigated: The ultrasonic pressure field is measured in high spatial resolution, and high speed videometry of occurring cavitation bubble structures and their respective effects on the membrane surfaces is carried out. The cleaning success is ascertained by permeability measurements and microscopy of the membrane surface.

Experimental arrangement

All investigations are done under most realistic conditions. Therefore a small scale laboratory test plant for water filtration has been built up. A simplified sketch of the setup is shown in Figure 1. In a retentate tank made from glass ($120 \times 50 \times 50\,\mathrm{cm}^3$) there are two ultrasound (US) transducers (Elma, Germany, 32×41 cm^2) that can operate at 35 kHz or 130 kHz with an overall power of 2000 W. Its power output is controlled from 10 % to 100 %. The retentate tank is filled with tap water with a soluted coagulant ($FeCl_3$) and soft-clay, composed of very small particles, mostly up to 3 µm. In between of the US-transducers the membrane module is located. It consists of parallelly stacked flat sheet polymer membranes (type UP-150 Microdyn-Nadir). The membrane module performs the water filtration in the following way: Under controlled pressures the permeate is sucked out from its inner side by a pump so that on the membrane outsides an observable filter cake develops. This filter cake is cleaned periodically by the use of ultrasound.

A top view of the geometry of the membrane module of five membrane sheets is given in Figure 2. High speed videometry is carried out with a Photron Fastcam APX-RS. The sound field is measured with a hydrophone Reson TC4038. It can be moved in planes along the membrane module as well as into the intermembrane spaces by a step motor (see Figure 1).

For a better relative time and spatial resolution of the bubble behaviour in the cleaning process, a frequency scaled model (see next section) of the membrane module was used apart from the test plant in a 25 kHz bath (similar transducer, Elma, Germany).

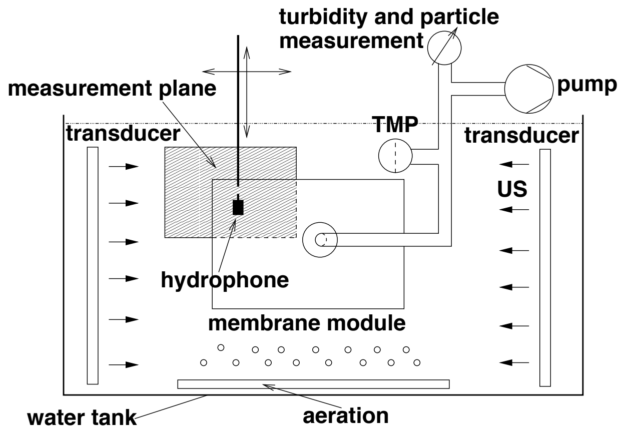

Figure 1: Sketch of filtration plant with the location of measurement planes in sideview.

Sound propagation

To describe the wave propagation mechanism an acoustic model of the membrane module was developed and its appropriability confirmed by optical observations and acoustic measurements, see [9]. A sketch of this model is given in Figure 2. The intermembrane

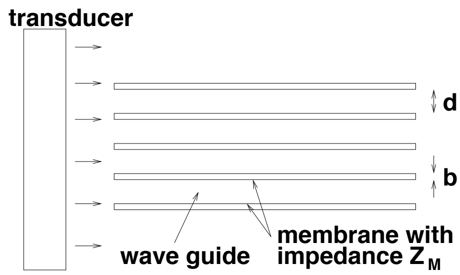

Figure 2: Acoustic model of the membrane module: The membrane sheets are of thickness b and the intermembrane spaces measure d.

spaces (distance d) are considered as softly bounded waveguides.

The geometry of the membrane module described above determines a critical frequency $f_c = c/2d$ for the acoustic wave to be propagable into the membrane module with the sound speed $c = 1480\,\mathrm{m/s}$ for water. All results presented here are obtained at a frequency above f_c.

In the following, the pressure field configurations as obtained by the hydrophone measurements are presented. For comparison, Figure 3 shows the color and height coded pressure field *without* the membrane module. The measurement plane is perpendicular to the transducers as indicated in Figure 1. The transducers are located vertically on the left and right and were driven at 130 kHz

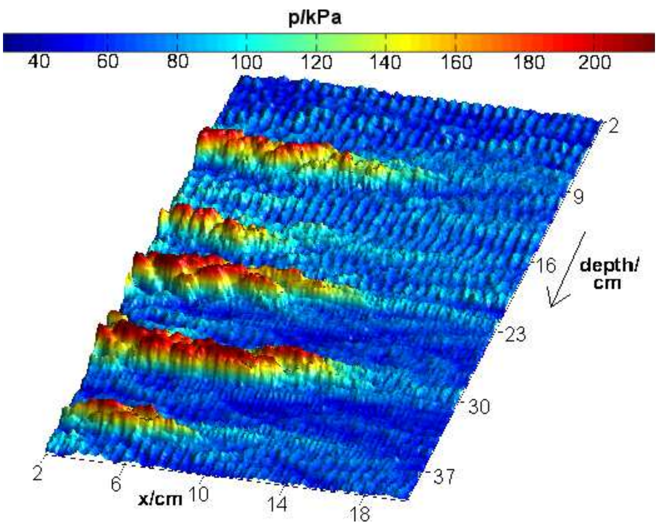

Figure 3: Pressure field with two transducers located at $x_1 = 0$ and $x_2 = 62$ cm running at $f_0 = 130$ kHz and $P = 20\,\%$. The x-axis gives the distance from the closer left transducer, the y-axis the depth below water surface level in cm.

with $P = 20\,\%$. A standing wave field of low amplitude for $\lambda_0 = c/f_0 = 1.12$ cm gets clearly visible. Especially in the lower part of the figure also a standing wave of $\lambda_0/2$ becomes observable. Most strikingly there are five horizontal structures of high pressure proceeding from the closer transducer on the left to the right. Note that the plane transducer is composed of several hexagonal piezo elements that determine the shape of the pressure field. Optical observations show the presence of streamers along the horizontal structures and obviously the sound pressure propagates preferably along them. A strong directivity in the sound propagation along a bubble chain was found and explained by Manasseh [6] with a simple model of spring-like coupled bubbles.

In Figure 4 the acoustic pressure in a plane as in 3 is presented with the membrane module submerged into the retentate tank. The membrane module is situated at the lower right corner delimited by the white line. The measurement cutouts show the acoustic pressure of about a quarter of an intermembrane space. From Figure 4 from top to bottom the evolution of the pressure field for increasing driving power from 10 % to 100 %, corresponding 200 W to 2000 W, can be observed. It turns out that at 10 % and 20 % a standing wave field evolves while the pressure field can be described linearly. Between 20 % and 25 % the pressure field configuration changes qualitatively: The medium becomes much more dissipative and the pressure in the intermembrane space even lowers despite of the augmenting driving power. Together with the lower sound pressures in the intermembrane space characteristic horizontal structures of higher pressure amplitude occur in front of the membrane module. They are modulated with a horizontal standing wave. Optical observations show that in front of the membrane module the cavitation bubble density is high and suggest that in the structures in front of the membrane module streamer of bubbles cross the measurement plane. The high

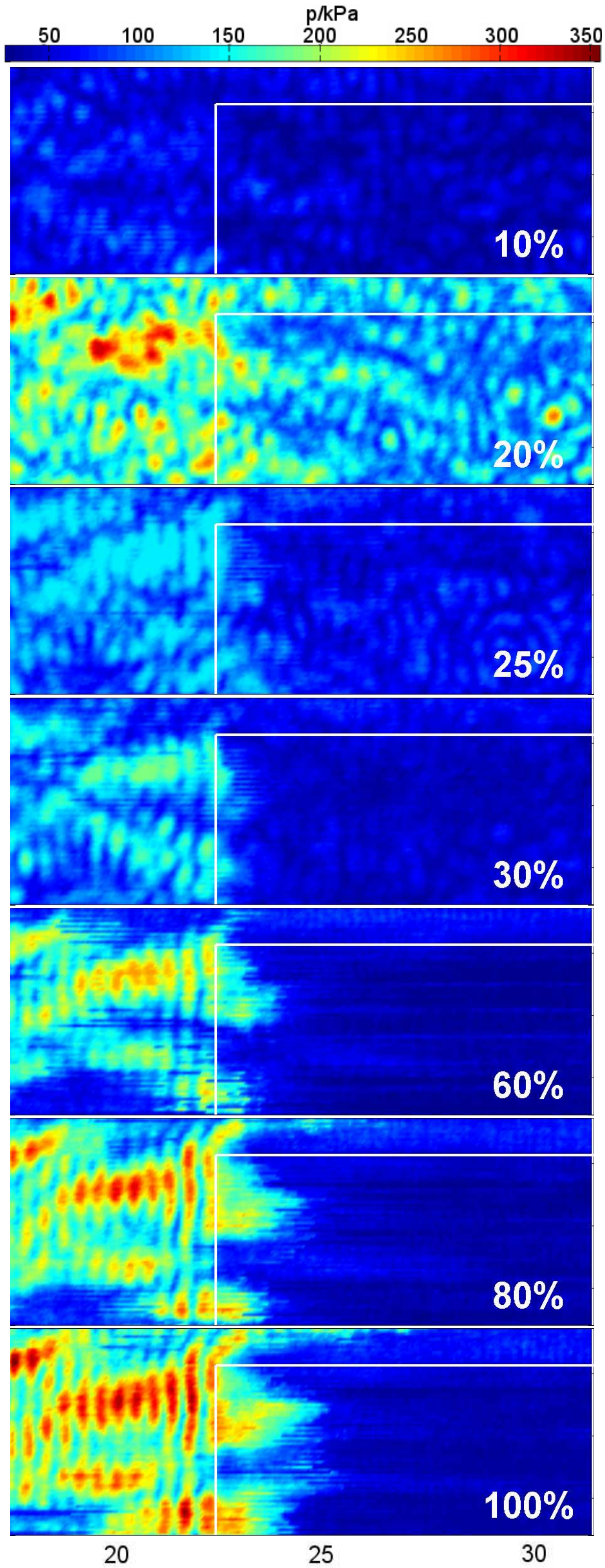

Figure 4: Evolution of the pressure field with raising driving power at 130 kHz. The two transducers are situated vertically, perpendicular to the paper plane left and right from the membrane module at $x_1 = 0$ and $x_2 = 65$ cm, respectively (compare Figure 1). They are driven at $f_0 = 130$ kHz. The measurement planes cover a section from -17 cm to -23 cm below the water surface. Axes in cm, the planes shown measure approximately $14 \times 6\,\text{cm}^2$.

pressure in front of the membrane module is due to reflection on the waveguides that are not impedance matched. Taking the ratio of the pressure in the inter-membrane spaces to the pressure outside as a measure for the efficiency of delivering sound pressure to the membrane surfaces, it is obvious that the efficiency lowers simultaneously with the occurrence of the structures in front of the membrane module. There are several explanations for this. One is that the bubble structures which occur at higher driving powers in front of the membrane module shadow the intermembrane space from the transducer. Another approach takes into account the sound conducting attributes of streamers, induced by self focussing or coupling between the bubbles (see Figure 3). As streamers avoid regions of higher pressure [1, 7, 8], like in front of the membrane module, they get deviated around the membrane module. This hinders self focussing into the membrane module. Obviously, in the sound propagation model of the bubble chain the sound pressure propagates preferably along the deviated streamers, thus neither into the membrane module.

Cleaning mechanisms

To be able to improve ultrasonic membrane cleaning systematically, a deeper understanding of the cleaning mechanisms must be obtained first. From optical observations it has been found that bubble movement on the membrane surface is closely linked to cleaning. The bubbles are created close to the transducer or in front of the membrane module between membrane module and transducer at the pressure maxima (see Figure 4). The following bubble movements can be observed to be dominant: The bubbles travel from their respective locations of creation into the intermembrane spaces. There they arrange to bubble layers that are located in the middle of each intermembrane space, parallel to the membrane sheets (see Figure 5 left). The bubble density of the layers as well as the number of bubbles on the membrane surfaces show a strong dependence on the acoustic power. As soon as the bubbles in the layers reach Minnaert resonance size, they are accelerated by primary Bjerknes forces towards the membrane surfaces identified as the locations of the sound field nodes (see acoustical model in the previous section). With their impingement on the membrane surface ($v \approx 0.4\,\mathrm{m/s}$) and their subsequent oscillations they can disrupt the covering cake layer and produce circular holes in the cake layer, as in the right picture of Figure 5 (green markers) shown. The picture gives a microscopic view onto the cake layer on the membrane surface. The cake layer appears orange, on the cleaned parts the view on the white membrane surface is revealed. Besides the cleaned areas with circular shape there are lanes of cleaned area visible (see the long irregular path in the center of Figure 5). The lanes are result of volume and surface oscillating bubbles that creep over the membrane surface. These bubbles mainly take course along the boundary of already existing holes of the cake layer or even creep beneath the cake layer. On their movement they get accelerated rather abruptly and for short times reach speeds of several m/s. It turns out that the creeping bubbles play a crucial role in cleaning. So the typical movement of a cleaning bubble along the membrane is shown in the two pictures from Figure 6. The pictures are taken from a high speed movie ($\nu = 5600\,\mathrm{fps}$, exposure time $T_{ex} = 1/\nu$) and show a view on a hole in the cake layer on the membrane surface (red marker). The membrane sheet is located on the right vertical edge of each picture. Apart from the existing hole within the red marker its surface is fouled and clogged by the cloudy-like cake layer. Creeping over the membrane surface along the cake layer edges, the oscillating bubble (blue marker) extends the already present hole. So fragments of the cake layer are removed (yellow markers). It can be estimated from further microscopic investigation that more than 90 % of the surface is cleaned by bubbles that move on paths over the membrane while less than 10 % of the cleaned surface is covered with circular holes from impinging or fixed bubbles. Whether a bubble (or a bubble cluster)

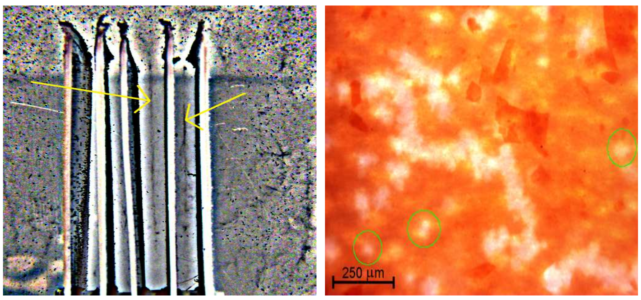

Figure 5: Left: View on the upper half of the membrane module with the transducer in the background in the paper plane and the bubble layers parallel to the membrane sheets visible. In this false color representation bubbles appear black. ($f_0 = 130\,\mathrm{kHz}$). **Right:** Microscopy of the membrane surface. The cake layer appears orange, cleaned areas white. The cleaned areas are in the form of circular holes (green markers) or longer lanes.

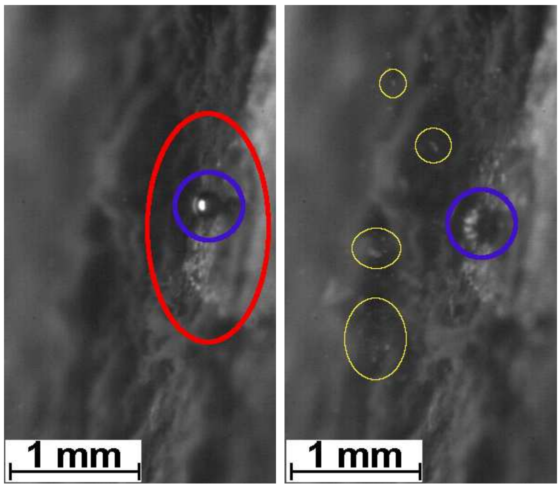

Figure 6: Two frames (exposure time 1/5600 s) separated by 225 ms. View on a hole (red marker) in the cake layer of the membrane. The membrane is located along the right vertical edge. A bubble (blue marker) moves and oscillates so that cake layer fragments (yellow marker) are removed. ($f_0 = 25\,\mathrm{kHz}$, $P = 100\,\%$)

stays in its place or starts moving over the membrane surface is determined, besides influence from secondary Bjerknes forces from neighboring bubbles, mainly by the size of the respective bubble compared to the ultrasonic frequency. This seems to be a result of the so determined energy the bubble can absorb from the sound field as well as the extremal distances a bubble gets from the membrane surface. When there is no ultrasound turned on, the contact angle between bubble and membrane is around 180°. This is due to the fact that the membrane surfaces are hydrophilised. This also affects the distance of oscillating bubbles from the surface and thereby the way of impingement of microstreams. In addition it is observed from the videometry that bubbles around the Minnaert radius are most important for cleaning while big bubbles with radii bigger than three or four times the Minnaert resonance radius do not play a significant role in cleaning.

Some strong erosive process is ought to be helpful to initially disrupt the cake layer, the more the more the membrane is fouled and covered by a biofilm. But most of the surface is cleaned by bubbles that travel over the membrane surface without showing any violent collapses or strong jetting. So from the videometry together with the result of the acoustic measurement that showed a sound pressure of around 50 kPa at the membrane surfaces, it can be concluded that the membrane, as a sound soft material, is cleaned by soft cavitation.

In the following the effects of a perpendicular alignment of the intermembrane spaces (the waveguides) to the transducer planes are compared to a parallel alignment. In the parallel alignment (the membrane module is rotated by 90° compared to Figure 2) two main problems occur: Only the outer membrane sheets opposite to the transducers (so the first and the last membrane sheet) get insonated while the sound pressure does not reach the other membrane surfaces. Furthermore, on the outer membranes bubbles traveling from the transducers impinge on the surfaces and may collapse violently. So after several hundreds of hours of sonication a sporadic damage of the membrane could be observed (see the circular hole in the middle of Figure 7 of about 100 μm diameter). In contrary, in the case of

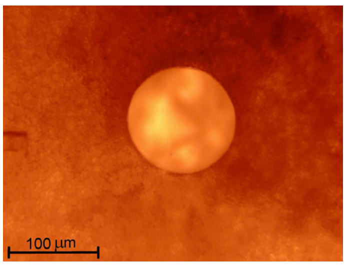

Figure 7: Microscopic investigation of damage on the membrane that can occur in the parallel alignment when the membrane is located very close to the transducer (insonication at 35 kHz and 130 kHz).

the perpendicular alignment (as sketched in Figure 2) bubbles are delivered well to the membrane surface and creep over it. Above all, by microscopic inspection of the membrane surface and particle counting as well as turbidity measurements of the permeate, in this arrangement even after thousands of ultrasound cycles the membrane integrity was ensured and no damage was found.

Conclusions

It was found that sound soft materials are mainly cleaned by soft cavitation. Furthermore it could be shown why subtle changes in geometric arrangement, variation of the membrane sheet distance or the alignment of the membrane module to the transducer can heavily affect the result. Some astonishing processes in sound propagation due to the presence of bubbles occurred and showed non-intuitive effects at raising the driving power. They should be investigated more deeply by sound field measurements and videometry.

References

[1] I. Akhatov, R. Mettin, C.-D. Ohl, U. Parlitz, W. Lauterborn: ‘Bjerknes force threshold for stable single bubble sonoluminescence’, Phys. Rev. E **55** (1997) 3747-3750

[2] D. Chen, L. K. Weavers, H. W. Walker: ‘Ultrasonic control of ceramic membrane fouling by particles: Effect of ultrasonic factors’, Ultrasonic **13** (2006) 379-387

[3] K. Kyaing Latt, T. Kobayashi: ‘Ultrasound-membrane hybrid process for enhancement of filtration properties’, Ultrasonic **13** (2006) 321-328

[4] H. Kyllönen, P. Pirkonen, M. Nyström, J. Nuortila-Jokinen, A. Grönroos: ‘Experimental Aspects of ultrasonically enhanced cross-flow membrane filtration of industrial wastewater’, Ultrasonic **13** (2006) 295-302

[5] S. Lauterborn, W. Urban: ‘Ultrasonic cleaning of submerged membranes for drinking water applications’, Proc. Acoustics ’08 Paris, Soc. Franc. d’Acoustique (ed.) **90** (2008) 2603-2608

[6] R. Manasseh, A. Nikolovska, A. Ooi and S. Yoshida: ‘Anisotropy in the sound field generated by a bubble chain’, Journal of Sound and Vibration **278** (2004) 807-823

[7] R. Mettin, S. Luther, C.-D. Ohl, W. Lauterborn: ‘Acoustic cavitation structures and simulations by a particle model’, Ultrasonic Sonochemistry **6** (1999) 25-29

[8] R. Mettin: ‘Bubble structures in acoustic cavitation’, Bubble Dynamics in Acoustic Fields: Modern Trends and Application, A. Doinikov (ed.), Research Signpost, Kerala, India, 2005, 1-36 (2005)

[9] F. Reuter, R. Mettin, W. Lauterborn: ‘Pressure fields and their effects in membrane cleaning applications’, Proc. Acoustics ’08 Paris, Soc. Franc. d’Acoustique (ed.) **90** (2008) 579-584